ISSN (Print) 1226-1750
ISSN (Online) 2233-6656
**Journal of Magnetics** 24(1), 17-23 (2019) https://doi.org/10.4283/JMAG.2019.24.1.017

# Performance of Magnetic Switching at the Recording Temperature in Perpendicularly Magnetized Nanodots

**Nur Aji Wibowo[1,4]*, Didit Budi Nugroho[2,4], and Cucun Alep Riyanto[3,4]**

*[1]Department of Physics, [2]Department of Mathematics, [3]Department of Chemistry, Faculty of Science and Mathematics, Universitas Kristen Satya Wacana, Indonesia*
*[4]Study Center for Multidisciplinary Applied Research and Technology, Universitas Kristen Satya Wacana, Indonesia, Jl. Diponegoro 52-60 Salatiga - Indonesia 50711*

(Received 23 November 2018, Received in final form 15 February 2019, Accepted 15 February 2019)

**A temperature-dependent micromagnetic study has been conducted to examine the spin dynamics of the perpendicularly magnetized nanodot in a thermally induced magnetic switching (TIMS) scheme. The magnetic parameters used in this study represent the properties of BaFe. The impact of writing-temperatures below the Curie point on the magnetization reversal characteristic of nanodot with three damping levels, which related to the minimum writing-field as well as the zero-field-switching probability, were discussed systematically. The spins configuration of the nanodot was also presented to visualize the modes of the magnetization switching. The simulation reveals that the writing-field decreases concerning with the writing-temperature and reaches its lowest value at the temperature of 0.4 % below its Curie point. During the heating phase, the mechanism of demagnetization is coupled with the writing-temperature. Meanwhile, the magnetic damping takes over the role in the magnetic switching mechanism during the freezing.**

**Keywords:** Magnetic switching, Writing-field, Writing-temperature, Nanodot, Probability, ZFS

## 1. Introduction

Hard-Disk Drive on the market today is produced with the perpendicular magnetic recording technology [1, 2]. However, due to the writing-field magnitude constraint, the capacity of this perpendicular magnetic recording medium is almost at its maximum limit. As well known, the size dimension of data storage units determines the storage capacity. Reduction of the storage unit size up to sub-nanometer will cause the magnetic polarization instability even at ambient temperature. The use of materials with substantial magnetic anisotropy can overcome this instability. However, the use of this material would require a large magnetic field in data writing. The limited availability of the required writing-field [3] raises the idea of using extra energy like a stimulant in the writing process. Along with the development of laser technology, the heat carried by the laser is believed to be one of the most enabling types of energy that can be used as a stimulant [4]. Therefore, the presence of thermally induced magnetic switching (TIMS) method is one of the most popular solutions to the writing-field constraint [5, 6]. This heat-based magnetic recording technology allows us to use the material with large magnetic anisotropy as magnetic recording media to achieve higher capacity.

In TIMS, information is written through short localized heating on the recording medium and stored while cooled to room temperature [7]. This heating is carried out at temperatures up to the Curie point to obtain the writing-field lower than the field generated by the write-head. Recent research results confirm that by heating below the Curie point and utilizing a low-field writer less than 1.7 kOe, the magnetic polarization of the nano-ferromagnetic can be reversed. In fact, in the last five years, several experimental results supported by simulation studies have indicated that magnetization reversal may occur with the aid of heat sourced from sub-picosecond laser pulses [8, 9]. This result brings even higher expectations of the realization of magnetic recording media that the process of data writing is enough to use laser pulse stimulation without having to use a low driven magnetic field.

However, the most fundamental problem in the develop-


*Corresponding author: Tel: +6282138148265
Fax: +62298-321212, e-mail: nurajiwibowo@gmail.com

ment of current TIMS technology is an acceptable understanding of the fundamental behavior and optimization of magnetization dynamics of storage units during heating and cooling processes [10, 11] because the use of thermal fields potentially leads to a mess system. The disorder of heat-induced system behavior causes many possible magnetization reversal modes that have an impact on the writing-field magnitude. The scale of the writing-temperature is essential throughout the magnetization process [12]. As the writing-temperature approaches the Curie temperature, the magnetization randomness becomes higher. Therefore, it is necessary to calculate the minimum temperature required to realize a magnetization reversal with a minimum or even no writing-field.

In this paper, both the optimum writing-field as well as the zero-field-switching probability at writing-temperatures below the Curie temperature will be investigated systematically through temperature-dependent micromagnetic simulations. In addition, the way in which the magnetization of the perpendicularly-magnetized-nanodot reversed will also be analyzed based on the configuration of the magnetic domains.

## 2. Numerical Method

The simulated magnetic material was assumed to be BaFe. The BaFe has numerous attributes suitable for use as high-density HDD material. It has strong magnetic anisotropy and also an excellent chemical endurance. Quantities representing the intrinsic magnetic properties of BeFe were based on the literature of Boardman [13], and Shirk and Buessem [14]. These quantities were magnetic saturation ($4\pi M_S$), perpendicular anisotropic constants ($K$), and exchange constant ($A$), with the respective values, were 4800 Gauss, $3 \times 10^6$ erg/cc, and $6.3 \times 10^{-7}$ erg/cm. Meanwhile, the Curie temperature ($T_C$) was taken at 740 K which the moderate size typically used in the

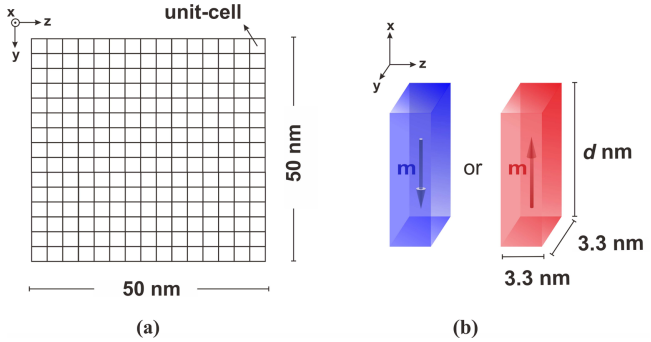


**Fig. 1.** (Color online) A simulated object which called as nanodot, (a) Surface view of the nanodot, (b) Colored unit-cells with the opposite spin orientation.

Heat-Assisted Magnetic Recording application [15].

The simulated storage unit was a ferromagnetic layer having an easy axis perpendicular to its surface which lies in the $yz$-plane. Figure 1 shows the idealization of the storage unit which referred to as the nanodot. This unit was assumed to be rectangular parallelepiped with a surface of 50 × 50 nm$^2$ (Fig. 1(a)) with a thickness $d$ which composed from 225 uniform unit-cells with each size of 3.3 × 3.3 × $d$ nm$^3$ (Fig. 1(b)). This lateral surface unit-cell size was set to be 3.3 nm in order to make it smaller than the magnetostatic exchange length, $l_{ex}$, which given by $(A/2\pi M_S^2)^{0.5}$ where $l_{ex}$ is in cm, $A$ is in erg/cm, and $M_S$ is in emu/cm$^3$ [16]. Based on the selected intrinsic magnetic properties ($A$ and $M_S$), $l_{ex}$ of the simulated nanodots is ~ 8.3 nm. To ensure stability of an initial equilibrium magnetization in data storage viewpoint, the energy barrier of the nanodot should be larger than 40 $k_B$T [17]. According to the pre-calculation, by counting the height between the maximum and minimum energy of the nanodot during exposed by the external magnetic field which its magnitude increase linearly from 0 to 2 Tesla for 2.5 ns, the energy barrier of nanodot with the thickness of 10 nm was obtained about 1800 $k_B$T. So that, in this study, the selected nanodot thickness was 10 nm.

These cells represented the smallest part of a storage unit that had only a magnetic spin. The direction of the arrow indicated the orientation of this spin. When the spin points to the (+$x$)-axis, the unit cell was red colored. While as the spin lies in the (–$x$)-axis, the unit cell was blue colored. The magnetic storage unit idealization was adopted from a model previously performed by Mizoguchi and Cargill III [18]. The adjacent spin cells interacted to produce an exchange field. This interaction affected the magnitude of the total magnetization of nanodot. In view as an entire storage disk, nanodot was assumed to be a data storage unit which presence was neither influence nor influenced by surrounding nanodots.

To find out the magnetization behavior of the storage unit in response to any applied pulses, whether of the magnetic field pulse and or the heat pulse, a temperature-dependent micromagnetic simulator was constructed based on the stochastic Landau-Lifshitz-Gilbert (LLG) equation. The simulators and algorithms used in this study were similar to those used by Purnama *et al.* [19, 20] in a previous study which was the work of Konishi *et al.* with modifications on the aspect of temperature [21]. The magnetic field that interacts with the magnetic moment of each spin was expressed as a resultant of the five field components, i.e., the demagnetization field, the anisotropy field, the exchange field between the adjacent spins, the external applied magnetic field, and the thermal field. The

first three mentioned fields were contributed by the intrinsic magnetic properties of materials represented by $M_S$, $K$, and $A$. They decrease with the increase of temperature. Based on the empirical approach proposed by Purnama *et al.* [19], the magnetic saturation of the ferromagnetic material in temperature effect, $M_S(T)$, was proportional to $(1 - T/T_C)^{0.5}$. While the temperature dependence of the anisotropy and the exchange constants, $K(T)$ and $A(T)$, can be assumed to follow a simple two-dimensional relationship of $M_S(T)$ [22] because the nanodot was simulated as a material which composed from many unit-cells. As for the thermal field, its magnitude fluctuates where the average value was assumed to be zero during the magnetization process. The distribution of this field was supposed to follow the Gaussian distribution equation which its coefficients determined by the Fluctuation-Dissipation Theorem proposed by Brown [23]. For optimization in the computation process, the integration step used was 0.25 ps.

Figure 2 illustrates the configuration of a double-pulse consisting of thermal field and magnetic field which was exposed to the nanodot. In this study, the simulation started with the presence of the magnetic field pulses. This field linearly raises from zero to its maximum value which called as inductor field, $H_w$. Shortly after that, the nanodot was locally heated by a thermal field pulse up to reach a peak temperature which referred to as the writing-temperature, $T_w$. The data writing period was performed during the heating phase with the time interval, $t_h$, was 1 ns. Whereas the data storage was carried out during the cooling phase to ambient temperature (298 K) with a time interval, $t_c$, was 0.5 ns. The cooling interval in this sub-nanosecond order was used to ensure that the nanodot freezes locally to ambient temperature [3]. These heating and cooling phases take place in the presence of $H_w$.

To calculate either the probability of reversal or the magnitude of the writing field, computation was completed by using twenty different random numbers that implemented at the magnetization value of the nanodot. Each calculation was performed on $H_w$ whose magnitude increases systemically from 0 Tesla up to a value which results in a complete reversal probability (i.e., reversal probability equal to one). This magnetic field was directed parallel to the (+)$x$-axis. The minimum magnetic field required to produce this fully magnetization reversal is called as a threshold field, $H_{th}$. This field can be associated with the field required to write data which called as the writing field. To obtain the information regarding the impact of temperature on the magnetization reversal characteristic, $T_w$ was varied from 722 K to 739.99 K. Each series of calculations was performed on three level of magnetic damping. The damping levels were quantized by assigning different Gilbert damping constant values ($\alpha$), i.e., 0.008, 0.10, and 0.20.

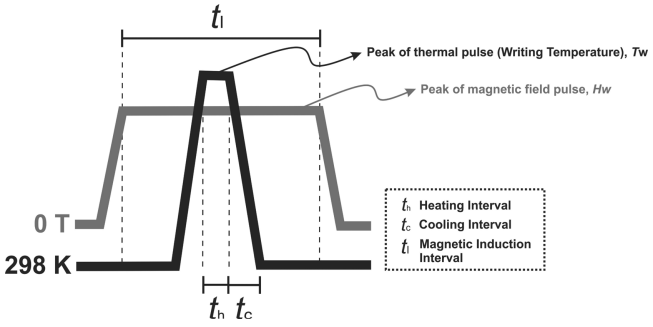


**Fig. 2.** Double-pulse structure. The solid grey line is the magnetic field pulse. Meanwhile, the solid black line is the thermal pulse.

## 3. Result and Discussion

Figure 3 shows the writing-temperature dependence of the writing field. The magnitude of the writing-field significantly influenced by the temperature of heating. As the temperature increases, the writing-field decreases. The more drastically decreasing of the field occurs at the nanodot with more considerable damping. Even though there is a difference in the rate of decrease, the writing field of the three different damped nanodot types eventually has the lowest magnitude when it reaches a temperature of 737 K. At this temperature, the writing-field of these nanodots are at least 30 mT, 25 mT, and 40 mT for nanodot with Gilbert damping value of 0.20, 0.10, and 0.08 respectively. At the writing-temperature interval $< 737$ K, the writing-field varies with respect to the writing-temperature by a factor of $(1 - \beta\, T_w/T_C)^{\gamma}$. Writing-field behavior as a function of writing-temperature refers

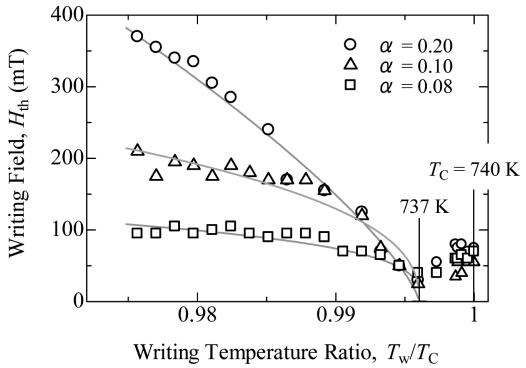


**Fig. 3.** Writing-field of the nanodot plotted as a function of writing-temperature ratio to the Curie temperature. Grey solid lines express the fitting curve: $H_{th}(T) = A\ (1 - \beta\, T_w/T_C)^{\gamma}$.

to a change of heated anisotropy constant as previously stated by Mansuripur *et al.* [22]. In this temperature interval, the energy of magnetic anisotropy, which is a manifestation of the interaction between electron spins and orbital moments (spin-orbit coupling), plays a significant role in the magnetic reversal dynamics. For this reason, the strength of the magnetic anisotropy can be controlled by means of the electronic structure modification. The spin-orbit coupling interaction is temperature dependent. This interaction depleted at an elevated temperature and touched its minimum at $T_w$ = 737 K. Depletion of spin-orbit interaction leads to writing field reduction which also reaches its minimum value at 737 K. While at intervals of 737 K < $T_w$ < 740 K, the magnitude of the writing-field tends to be random in the range of tens of milli-tesla. The electrons with high temperature can effectively stimulate the magnetic switching [24]. At this interval, role domination of spin-orbit coupling interaction in magnetic reversal process is replaced by a thermal fluctuation field. Effect of fluctuations due to heat at the given temperature causes this randomization. These fluctuations occur in entire constituent fields, i.e., the demagnetization fields, the anisotropy fields, the exchange fields, and the applied magnetic fields.

Figure 4 expresses the normalized magnetization value, $M$, on the three writing-temperatures of the nanodot with three different damping levels. The three writing-temperatures presented are 724 K, 737 K, and 739 K. Each of these temperatures represents the following data: $T_w$ < 737 K, $T_w$ = 737 K, and 737 K < $T_w$ < 740 K. Initially, the nanodot magnetization is saturated with a (−$x$)-axis polarization characterized by $M$ = −1. In the early several hundred picoseconds since the external magnetic field was applied, the magnetic polarization does not alter even exposed by a magnetic field in the (+$x$)-axis direction. Polarization begins to turn shortly after a thermal pulse is given. During the heating phase, in $t_h$ intervals, the varies of magnetization takes place in several ways which heavily depend on $T_w$. At $T_w$ < 737 K, for entire damping levels, the demagnetization process takes place through the nucleation of a domain-wall. There is a different domain-wall pattern between weak and strong damped nanodot. At nanodot with 0.08 of damping constant, a straight domain-wall is nucleated along the diagonal of the surface plane. While at nanodot with 0.10 and 0.20 of damping constant, a curved domain-wall is nucleated from one-end of diagonal. These wall patterns observed from the visualization of the unit-cells spin configuration of the nanodot in Fig. 5(a) [$a_{h1}$, $b_{h1}$, $c_{h1}$]. While in the range 373 K ≤ $T_w$ < 740 K, demagnetization takes place through randomization of the unit-cells spin (or often

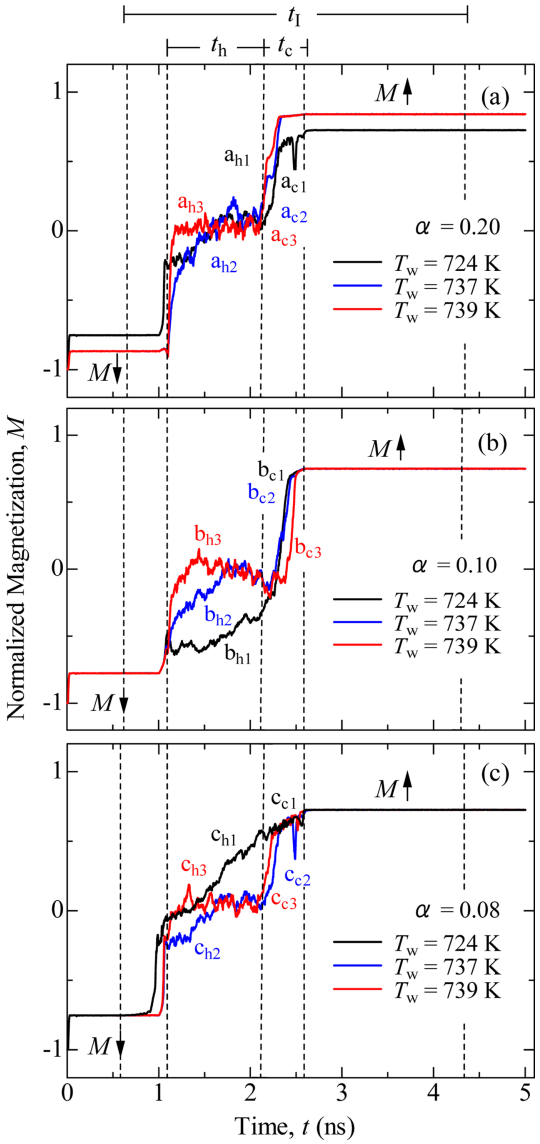


**Fig. 4.** (Color online) The normalized magnetization of nanodot under double-pulse presence.

referred to as multi-domain configuration) as shown in Fig. 5(a) [$a_{h2}$, $a_{h3}$, $b_{h2}$, $b_{h3}$, $c_{h2}$, $c_{h3}$].

In Fig. 4 and Fig. 5(b) also observed that during the phase of cooling (in the $t_c$ interval), damping level plays two important roles in the magnetization switching mode. The first, the magnetic damping takes a response for controlling the speed in achieving a complete magnetic switching parallel to the magnetic field induction. Along with the increased damping, the nanodot will be magnetized faster towards the field before the cooling phase expired. While at low damping ($\alpha$ = 0.08), the perfect magnetic reversal occurs to coincide with the end of the cooling phase. The second, the magnitude of the magnetic damping determines the mode of the magnetization

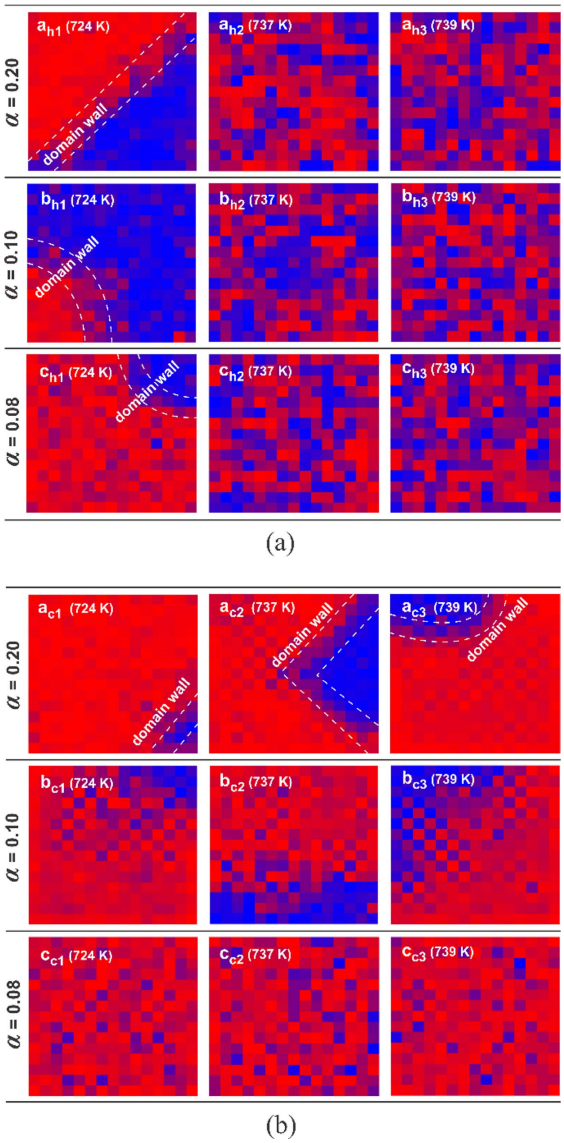


**Fig. 5.** (Color online) Unit-cells spin configurations of the nanodot, (a) while heating, (b) while freezing.

reversal. In Fig. 5(b) [$a_{c1}$], at the strongly damped nanodot with 724 K of $T_w$, the magnetization switching process takes place through the propagation of the domain-wall that has been nucleated since the heating phase started. Whereas from Fig. 5(b) [$a_{c2}$, $a_{c3}$] observed that in nanodots with the equal damping level nevertheless with two different $T_w$ (737 K and 739 K), domain-walls was formed despite already preceded multi-domain configuration in the previous phase. Nucleation process of this wall was followed by the propagation process until the magnetization of the nanodot completely lies in the direction of the applied magnetic field. As the magnetic damping weakens, the magnetization switching mode is no longer dominated by the nucleation and propagation of the

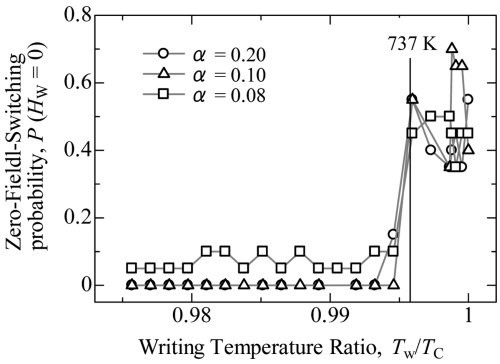


**Fig. 6.** The zero-field-switching probability of the nanodot.

domain-wall but begins to be replaced by multi-domain configuration mode. Even the nucleation and propagation of the domain-wall mode does not arise at all in the weak-damped nanodot as seen from the Fig. 5(b) [$c_{c1}$, $c_{c2}$, $c_{c3}$].

The phenomenon of magnetization switching only with the support of a thermal pulse (the magnetic field is switched off) or often stated to as zero-field-switching (ZFS) is also observed in this simulation study. The ZFS is observed from the non-zero probability of the reversed magnetization of the heated nanodot even though the applied magnetic field is removed, $P$ ($H_w$ = 0). Figure 6 shows the magnitude of the ZFS probability. For the writing-temperature less than 737 K, occurrences of ZFS are infrequently observed. Even at the damping value of 0.20 and 0.10, ZFC is completely unnoticed. However, ZFS is frequently detected in the entire modeled nanodots when the writing-temperature rises to within 373 K $\leq T_w$ < 740 K. Even in that temperature range, the probability of ZFS is in the range of 35-70 %. $T_w$ = 373 K is the critical temperature at which the magnetic anisotropy energy reaches its minimum level. At this temperature, the thermal fluctuation field has overtaken the control. The elevated thermal energy advantages to a high energy transfer [25], causes the energetically spin system which leads into a disordered spins state [26]. The substantial increase of ZFS probability within 373 K $\leq T_w$ < 740 K is correlated to the effect of the annihilation of two domain walls replaced by the magnetic spins randomization during the heating phase through the configuration of multi-domains. The transformation mode from domain wall nucleation to multi-domain configuration could be associated with the rapid decrease of the domain-wall energy at temperatures close to the Curie temperature which previously studied by Vértesy [27]. It was caused by the reduction of the interaction energy between the adjacent unit-cells with the increasing temperature. The ZFS phenomena are believed could be a crucial property in designing the low power spintronic devices [28] even though its

occurrence had not theoretically expected by the scientists [29].

## 4. Conclusion

A temperature-dependent micromagnetic investigation has been performed on the dynamics of magnetization reversal of the perpendicularly magnetized nanodot with either induced magnetic fields or only with thermal pulses. The essential results are summarized below:

1) The magnitude of the writing-field decreases with the writing-temperature and reaches its lowest value at a precise temperature 0.4 % below its Curie point.

2) In fact, at certain writing-temperatures, the probability of the magnetization to completely reverse without an induced magnetic field at a damped nanodot is increased drastically up to 55 %.

3) The simulation results also reveal that during the heating phase, the demagnetization mechanism depends on the writing-temperature. At low temperatures, demagnetization occurs through the formation of a domain-wall. While at high temperatures (close to the Curie point), multi-domain configuration plays as the main ways during demagnetization.

4) During the cooling phase, the magnetic ordering towards the opposite polarization is no longer controlled by temperature but by the magnetic damping, where the multi-domain configuration mode is gradually replaced by the domain-wall nucleation as the magnetic damping enlarged.

5) During the cooling phase, the magnetization reversal is held in a shorter time as the magnetic damping enlarged.

## References

[1] S. Iwasaki, J. Magn. Magn. Mater. **324**, 3 (2012). [DOI]: 10.1016/j.jmmm.2010.11.092

[2] S. N. Piramanayagam, in 2010 APMRC, pp. 1-2 (2010). [URL]: https://ieeexplore.ieee.org/document/5682227

[3] U. Kilic, G. Finocchio, T. Hauet, S. H. Florez, G. Aktas, and O. Ozatay, Appl. Phys. Lett. **101**, 25 (2012). [DOI]: 10.1063/1.4772486

[4] P. Taptimthong, J. F. Düsing, L. Rissing, and M. C. Wurz, Procedia Technology **26**, (2016). [DOI]: 10.1016/j.protcy.2016.08.011

[5] O. Ozatay, T. Hauet, S. H. Florez, J. A. Katine, A. Moser, J.-U. Thiele, L. Folks, and B. D. Terris, Appl. Phys. Lett. **95**, 17 (2009). [DOI]: 10.1063/1.3250924

[6] T. W. McDaniel, J. Appl. Phys. **112**, 1 (2012). [DOI]: 10.1063/1.4733311

[7] C. J. Sun, D. B. Xu, D. L. Brewe, J. S. Chen, S. M. Heald, and G. M. Chow, IEEE Trans. Magn. **49**, 6 (2013). [DOI]: 10.1109/TMAG.2013.2248055

[8] S. Gerlach, L. Oroszlany, D. Hinzke, S. Sievering, S. Wienholdt, L. Szunyogh, and U. Nowak, Phys. Rev. B. **95**, 22 (2017). [DOI]: 10.1103/PhysRevB.95.224435

[9] C. Xu, T. A. Ostler, and R. W. Chantrell, Phys. Rev. B **93**, 5 (2016). [DOI]: 10.1103/PhysRevB.93.054302

[10] G. Ju, Y. Peng, E.K.C. Chang, Y. Ding, A.Q. Wu, X. Zhu, Y. Kubota, T. J. Klemmer, H. Amini, L. Gao, Z. Fan, T. Rausch, P. Subedi, M. Ma, S. Kalarickal, C. J. Rea, D. V. Dimitrov, P. Huang, K. Wang, X. Chen, C. Peng, W. Chen, J. W. Dykes, M. A. Seigler, E. C. Gage, R. Chantrell, and J. Thiele, IEEE Trans. Magn. **51**, 11 (2015). [DOI]: 10.1109/TMAG.2015.2439690

[11] N. A. Wibowo and S. Trihandaru, J. Phys.: Conf. Ser. **776**, 1 (2016). [DOI]: 10.1088/1742-6596/776/1/012027

[12] C. Spezzani, F. Vidal, R. Delaunay, M. Eddrief, M. Marangolo, V. H. Etgens, H. Popescu, and M. Sacchi, Sci. Rep. **5**, 8120 (2015). [DOI]: 10.1038/srep08120

[13] R. P. Boardman, Ph.D. Thesis, University of Southampton, England (2005). [URL]:http://eprints.soton.ac.uk/45942/

[14] B. T. Shirk and W. R. Buessem, J. Appl. Phys. **40**, 3 (1969). [DOI]: 10.1063/1.1657636

[15] Y. Wang, T. Tanaka, and K. Matsuyama, AIP Adv. **7**, 5 (2017). [DOI]: 10.1063/1.4975490

[16] G. S. Abo, Y. Hong, J. Park, J. Lee, W. Lee, and B. Choi, IEEE Trans. Magn. **49**, 8 (2013). [DOI]: 10.1109/TMAG.2013.2258028

[17] M. Yi, H. Zhang, and B.-X. Xu, NPJ COMPUT **MATER**. **3**, 1 (2017). [DOI]: 10.1038/s41524-017-0043-x

[18] T. Mizoguchi and G. S. Cargill III, J. Appl. Phys. **50**, 5 (1979). [DOI]: 10.1063/1.326303

[19] B. Purnama, M. Koga, Y. Nozaki, and K. Matsuyama, J. Magn. Magn. Mater. **321**, 9 (2009). [DOI]: 10.1016/j.jmmm.2008.12.003

[20] B. Purnama, Y. Nozaki, and K. Matsuyama, J. Magn. Magn. Mater. **310**, 2 (2007). [DOI]: 10.1016/j.jmmm.2006.10.988

[21] N. A. Wibowo, F. S. Rondonuwu, and B. Purnama, J. Magn. **19**, 3 (2014). [DOI]: 10.4283/JMAG.2014.19.3.237

[22] M. Mansuripur and G. a. N. Connell, J. Appl. Phys. **55**, 8 (1984). [DOI]: 10.1063/1.333298

[23] W. F. Brown, Phys. Rev. **130**, 5 (1963). [DOI]: 10.1103/PhysRev.130.1677

[24] Z. Fu, Z. Zhang, and Y. Liu, SPIN, **08**, 03 (2018). [DOI]: 10.1142/S2010324718500145

[25] T.A. Ostler, J. Barker, R. F. L. Evans, R. W. Chantrell, U. Atxitia, O. Chubykalo-Fesenko, S. El Moussaoui, L. Le Guyader, E. Mengotti, L. J. Heyderman, F. Nolting, A. Tsukamoto, A. Itoh, D. Afanasiev, B. A. Ivanov, A. M. Kalashnikova, K. Vahaplar, J. Mentink, A. Kirilyuk, Th. Rasing, and A. V. Kimel, Nature Communications **3**, 666 (2012). [DOI]: 10.1038/ncomms1666

[26] X. Jiao, Z. Zhang, and Y. Liu, SPIN, **06**, 01 (2016). [DOI]: 10.1142/S201032471650003X

[27] G. Vértesy and I. Tomáš, J. Appl. Phys. **93**, 7 (2003).

[DOI]: 10.1063/1.1559434
[28] R. Materese, "Zero Field Switching (ZFS) Effect in a Nanomagnetic Device," NIST, Mar-2018. [URL]: https://www.nist.gov/topics/materials/zero-field-switching-zfs-effect-nanomagnetic-device. [Accessed: 21-Nov-2018].
[29] L. Saccone, "Nanomagnetic Devices and the Zero Field Switching Effect," In Compliance Magazine, 22-Mar-2018. [URL]: https://incompliancemag.com/nanomagnetic-devices-and-the-zero-field-switching-effect/. [Accessed: 21-Nov-2018]